Associative Properties in Water of Copolymers of Sodium 2-(Acrylamido)-2-methylpropanesulfonate and Methacrylamides Substituted with Alkyl Groups of Varying Lengths

Hiroshi Yamamoto, Itsuro Tomatsu, Akihito Hashidzume, and Yotaro Morishima*

Department of Macromolecular Science, Graduate School of Science, Osaka University, Toyonaka, Osaka 560-0043, Japan

Received December 7, 1999; Revised Manuscript Received August 7, 2000

ABSTRACT: Associative properties of random copolymers of sodium 2-(acrylamido)-2-methylpropanesulfonate (AMPS) with *N*-hexylmethacrylamide (C_6MAm) and with *N*-octadecylmethacrylamide (C_{18}MAm) in aqueous solutions were investigated comparing with those of AMPS copolymers with *N*-dodecylmethacrylamide (C_{12}MAm) reported previously. For characterization by fluorescence, all the polymers were labeled with 1 mol % of naphthalene by terpolymerization using *N*-(1-naphthylmethyl)methacrylamide. The polymers possessing C_6 or C_{12} alkyl chains exhibit a strong tendency for intramolecular hydrophobic association to form unimolecular micelles when the C_nMAm (n = 6, 12) contents in the polymers are in the ranges of 30−70 and 10−50 mol % for the C_6 and C_{12} chains, respectively. A similar tendency was observed for the polymers possessing C_{18} chains when the C_{18}MAm contents are in the range of 5−20 mol %, but polymer micelles formed were not completely unimolecular. Both the lower and upper limits of the C_nMAm contents for all the three polymers decrease significantly with increasing the length of the alkyl chain. When the C_nMAm contents are either lower or higher than these limits, the polymer-bound alkyl chains undergo interpolymer associations. Fluorescence depolarization and ^{1}H NMR relaxation times indicate that local motions of naphthalene labels and alkyl chains are more pronouncedly restricted in hydrophobic domains formed by longer alkyl chains. An inclination to the self-association of these polymers was discussed in terms of the ratio of the total number of carbon atoms in hydrophobes to the number of SO_3^- in a polymer chain. A conclusion is that with C_6 chains one needs to incorporate more carbon atoms into a polymer than with C_{12} and C_{18} chains to attain the same extent of hydrophobe associations. In other words, the CH_2 and CH_3 residues in the C_6 chain are much less effective than those in the C_{12} and C_{18} chains for the self-association when compared at the same hydrophobe/charge ratio in a polymer chain, whereas there is no significant difference between those in the C_{12} and C_{18} chains. Thus, the ability of the C_6, C_{12}, and C_{18} chains per carbon atom to associate is in the order $C_{18} \geq C_{12} \gg C_6$.

Introduction

Hydrophobically modified water-soluble polymers have been a target of extensive studies in the past decades because of their potential in industrial applications such as water-borne paints, coating fluids, cosmetics, foodstuff, drug delivery systems, oil recovery, and water treatment and also because of their relevance to biological macromolecular systems.[1−6]

In amphiphilic polyelectrolytes, hydrophobic interactions among hydrophobic residues compete with repulsive electrostatic interactions among charged segments in aqueous solution, resulting in the formation of various types of micellelike nanostructures. The self-association behavior of amphiphilic random copolymers can be controlled by molecular architectures which include the sequence distribution of hydrophilic and hydrophobic monomer units,[7−12] the spacer bond between hydrophobes and the polymer backbone,[13−16] and the type of hydrophobes and their content in the polymer.[13,17−21] The type of micellelike nanostructures is greatly different depending on whether hydrophobe associations occur in an intra- or interpolymer fashion in aqueous solution. Highly preferential intrapolymer associations lead to the formation of single-macromolecular or unimolecular micelles, whereas interpolymer associations yield network structures, giving rise to "thickening" phenomena. For example, random copolymers of sodium 2-(acrylamido)-2-methylpropanesulfonate (AMPS) and methacrylamides substituted with bulky hydrophobes at the N-position, in which hydrophobes are linked to the polymer backbone via an amide spacer bond, show a strong preference for intrapolymer associations in water.[17,22,23] As a result, they form compact unimolecular micelles even at high polymer concentrations. In contrast, random copolymers of AMPS and a hydrophobic methacrylate, in which hydrophobes are linked via an ester spacer bond, show a tendency for interpolymer associations even in dilute polymer solutions, resulting in the formation of multipolymer micellelike aggregates.[15,16]

Previously, we reported on the self-association behavior of copolymers of AMPS and methacrylamide N-substituted with a C_{12} alkyl chain (C_{12}MAm) characterized by various techniques including fluorescence (lifetime, depolarization, quenching, and nonradiative energy transfer) using polymers labeled with pyrene and/or naphthalene, viscosity, gel permeation chromatography (GPC), static light scattering (SLS), quasielastic light scattering (QELS), and ^{1}H NMR relaxation times.[22−24] The self-associative properties of these copolymers were found to be a strong function of C_{12}MAm content (f_{C12}) in the copolymer. When f_{C12} was lower than ca. 10 mol %, the polymer adopted a relatively open chain conformation, but there was a weak tendency for interpolymer association, giving rise to hydrophobically cross-linked chains depending on the polymer concentration.[25] In the range $10 < f_{C12} < 50$ mol %, the copolymers showed a strong tendency for intrapolymer

10.1021/ma9920487 CCC: $19.00
Published on Web 09/23/2000

Chart 1

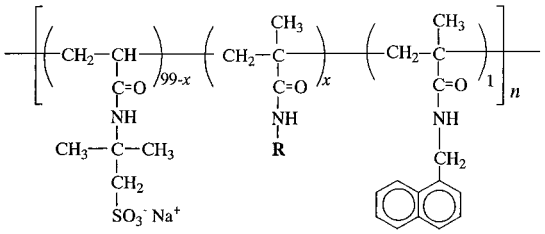

R = $-(CH_2)_5CH_3$ (C_6) : $x = f_{C6} = 0 - 80$ mol %

$-(CH_2)_{11}CH_3$ (C_{12}) : $x = f_{C12} = 0 - 60$ mol %

$-(CH_2)_{17}CH_3$ (C_{18}) : $x = f_{C18} = 0 - 40$ mol %

hydrophobe associations, leading to the formation of unimolecular micelles. However, when f_{C12} exceeded 50 mol %, multipolymer aggregates were formed, and all polymer chains were found in the aggregate with no unimolecular micelles coexisting.[23]

The association properties of the polymer should depend on the length of the alkyl chain, i.e., hydrophobicity, and also on the hydrophobe/charge ratio in a polymer chain, i.e., the ratio of the total number of carbon atoms (methylene and methyl groups) in alkyl substituents and AMPS charges in a polymer chain. Thus, it is important to elucidate how the "effectiveness" of the hydrophobe to cause the polymer to micellize depends on the length of the alkyl chain when the hydrophobe/charge ratios are the same.

In this work, we synthesized copolymers of AMPS with *N*-hexylmethacrylamide (C_6MAm) with the contents of C_6MAm (f_{C6}) ranging 0−80 mol % and also copolymers of AMPS with *N*-octadecylmethacrylamide (C_{18}MAm) with C_{18}MAm contents (f_{C18}) ranging 0−40 mol %. These copolymers were labeled with naphthalene (1 mol %) for fluorescence studies (Chart 1). We mainly focused on the association behavior of the AMPS-C_6MAm copolymers as characterized using fluorescence decay and depolarization, FT-IR, ^{1}H NMR relaxation, and QELS techniques. To discuss the effects of the length of the alkyl chain among C_6, C_{12}, and C_{18} chains in a systematic manner, characterization data for the AMPS-C_6MAm copolymers were compared with those for the AMPS-C_{18}MAm copolymers and also with those for the AMPS-C_{12}MAm copolymers obtained in our earlier studies.[22−24]

Experimental Section

Monomers. *N*-Hexylmethacrylamide (C_6MAm) was synthesized from hexylamine (Tokyo Chemical Industry Co.) and methacryloyl chloride (Tokyo Chemical Industry Co.) in a manner analogous to the synthesis of *N*-dodecylmethacrylamide (C_{12}MAm) as reported previously.[26] C_6MAm was purified by distillation under reduced pressure: yield 73.2%; bp 77−78 °C (at 0.2 mmHg). ^{1}H NMR (270 MHz, $CDCl_3$): δ 0.9 (t, 3H), 1.3−1.5 (m, 8H), 2.0 (m, 3H), 3.3 (q, 2H), 5.3 (m, 1H), 5.6 (s, 1H), and 5.9 (s, 1H). Anal. Calcd for $C_{10}H_{19}NO$: C, 70.96; H, 11.31; N, 8.27. Found: C, 70.44; H, 11.23; N, 8.16.

N-Octadecylmethacrylamide (C_{18}MAm) was synthesized from octadecylamine (Sigma-Aldrich Co.) and methacryloyl chloride in a manner analogous to the synthesis of C_{12}MAm. The crude product was recrystallized twice from ethanol and dried in vacuo at room temperature overnight: yield 65.8%; mp 65−66 °C. ^{1}H NMR (270 MHz, $CDCl_3$): δ 0.9 (t, 3H), 1.3−1.5 (m, 32H), 2.0 (m, 3H), 3.3 (q, 2H), 5.3 (m, 1H), 5.6 (s, 1H), and 5.9 (s, 1H). Anal. Calcd for $C_{22}H_{43}NO$: C, 78.27; H, 12.84; N, 4.15. Found: C, 78.08; H, 12.79; N, 4.22.

N-(1-Naphthylmethyl)methacrylamide (1NpMAm) was synthesized as reported previously.[27] 2-(Acrylamido)-2-methylpropanesulfonic acid (AMPS) was purchased from Wako Pure Chemicals and used without further purification. 2,2′-Azobis(isobutyronitrile) (AIBN) (Wako Pure Chemicals) was recrystallized twice from ethanol prior to use.

Terpolymerization. A general procedure for the preparation of naphthalene-labeled polymers is as follows: A mixture of AMPS, an alkylmethacrylamide, 1 mol % of 1NpMAm, and 0.1 mol % (based on the total monomers) of AIBN were dissolved in distilled *N*,*N*-dimethylformamide (DMF) in a glass ampule. The mole percents of the alkylmethacrylamides employed were 0−80 mol % for C_6MAm and 0−40 mol % for C_{18}MAm. The ampule was outgassed by six freeze−pump−thaw cycles on a vacuum line before sealing. The sealed ampule was immersed in a temperature-controlled water bath at 60 °C for 12 h. The reaction mixture was poured into excess ether to precipitate polymers. The polymer was purified by reprecipitation from a methanol solution into excess ether three times and then dissolved in a dilute aqueous NaOH solution. The aqueous solution was dialyzed against pure water for a week and finally lyophilized. The compositions of the terpolymers were determined by elemental analysis (N/C ratios) and UV absorption spectroscopy.

Other Materials. KBr (IR spectroscopy grade), NaCl, and $LiClO_4$ were purchased from Wako Pure Chemicals and used without further purification. Water purified with a Millipore Milli-Q system was used for all measurements.

Measurements. a. GPC. Measurements were performed at 40 °C with a JASCO GPC-900 equipped with Shodex Asahipak GF-7M HQ columns in combination with a JASCO UV-975 detector. A methanol solution containing 0.2 M $LiClO_4$ was used as eluent at a flow rate of 1 mL/min. Molecular weights of the polymer samples were calibrated with poly(ethylene oxide) standard samples purchased from Scientific Polymer Products.

b. Absorption and Fluorescence Spectra. Absorption spectra were recorded with a JASCO V-550 spectrophotometer. Steady-state fluorescence spectra were measured on a Hitachi F-4500 fluorescence spectrophotometer using a 1 cm path length quartz cuvette with excitation at 290 nm.

c. FT-IR. IR spectra were taken with KBr pellets on a JASCO FT/IR-410 spectrophotometer. The KBr pellets were prepared with polymer samples recovered from their aqueous solutions by a freeze-drying technique.

d. Fluorescence Lifetime. Fluorescence decays were measured by a time-correlated single-photon counting technique using a Horiba NAES-550 system equipped with a flash lamp filled with H_2. Sample solutions were excited at 290 nm and monitored with a cutoff filter (HOYA UV32) placed between the sample and detector. Both decay and response functions were measured simultaneously. Decay data were analyzed by a conventional deconvolution technique.

e. Fluorescence Depolarization. Fluorescence anisotropy (r) was measured on a Hitachi F-4500 fluorescence spectrophotometer equipped with a polarizer (excitation side) and an analyzer (detection side).[23] Fluorescence spectra for the naphthalene-labeled polymers were obtained at 25 °C by excitation at 290 nm and monitored at 325 nm. Both the excitation and emission slit widths were maintained at 10.0 nm. The r value was calculated from

$$r = (I_{vv} - gI_{vh})/(I_{vv} + 2gI_{vh}) \quad (1)$$

where I_{vv} and I_{vh} are the fluorescence intensities measured with parallel and perpendicular orientations of the excitation and emission polarizers, respectively, and g is the factor for instrumental correction (i.e., $g = I_{hv}/I_{hh}$). The rotational correlation time (τ_ϕ) was calculated from[28]

$$r_0/r = 1 + 3\tau/\tau_\phi \quad (2)$$

where r_0 is the limiting value of r for steady-state fluorescence in rigid media where no rotation occurs and τ is the fluores-

cence lifetime. The value of r for 1NpMAm in glycerol measured at 265 K (i.e., $r = 0.18$) was used as a value for r_0. This value was in agreement with that obtained by time-resolved fluorescence depolarization measurement.[23]

f. ^{1}H NMR Relaxation Times. ^{1}H NMR spectra were recorded with a JEOL EX-270 spectrometer using a deuterium lock at a constant temperature of 30 °C during the whole run. Sample solutions of 1.0 mg/mL polymer in D_2O containing 0.05 M NaCl were deaerated in NMR tubes by purging with Ar gas for 30 min prior to measurement. Proton spin−lattice relaxation times (T_1) were determined using a conventional inversion−recovery technique with a 180°−τ−90° pulse sequence.[29−31] Proton spin−spin relaxation times (T_2) were determined by the Carr−Purcell−Meiboom−Gill (CPMG) method using a $\{90°_x\tau(180°_y2\tau)_n\}$ pulse sequence.[32]

g. Quasielastic Light Scattering (QELS). QELS data were obtained at 25 ± 0.1 °C using an Otsuka Electronics Photal DLS-7000 light scattering spectrometer equipped with an Ar laser lamp (60 mW at 488 nm) and detector optics. An ALV-5000E digital multiple-τ correlator (Langen-GmbH) was employed for data collection. The autocorrelation function was measured at different angles (50°−130°). Sample solutions were filtered with a 0.2 μm pore size membrane filter prior to measurement.

The observed intensity autocorrelation function, $g^{(2)}(t)$, was measured experimentally, which is related to normalized autocorrelation function, $g^{(1)}(t)$, by the Siegert relation

$$g^{(2)}(t) = B[1 + \beta|g^{(1)}(t)|^2] \tag{3}$$

where β is a constant parameter for an optical system and B is a baseline term. To obtain the relaxation time distribution, $\tau A(\tau)$, the inverse Laplace transform (ILT) analysis for $g^{(2)}(t)$ was performed by conforming the REPES algorithm,[33] according to the equation

$$g^{(1)}(t) = \int \tau A(\tau) \exp(-t/\tau)\, \mathrm{d} \ln \tau \tag{4}$$

where τ is the relaxation time. The relaxation time distributions are given as a $\tau A(\tau)$ vs log τ profile with an equal area.

The translational diffusion coefficient, D, are calculated from ILT moments as

$$D = (\Gamma/q^2)_{q\to 0} \tag{5}$$

where Γ is the relaxation rate and q represents the magnitude of scattering vector expressed as

$$q = \frac{4\pi n}{\lambda} \sin(\theta/2) \tag{6}$$

where θ is the scattering angle and n is the refractive index of the solution. The hydrodynamic radius, R_h, is given by the Einstein−Stokes equation

$$R_h = \frac{k_B T}{6\pi\eta D} \tag{7}$$

where k_B is the Boltzmann constant, T is the absolute temperature, and η is the solvent viscosity. The details of QELS instrumentation and theory are described in the literature.[34,35]

h. Static Light Scattering (SLS). SLS data were obtained at 25 °C with an Otsuka Electronics Photal DLS-7000 light scattering spectrometer equipped with an Ar laser (50 mW at 488 nm). Sample solutions of polymers in 0.2 M NaCl were filtered with a 0.2 μm pore size membrane filter prior to measurement. The details of SLS measurements and data analysis are described elsewhere.[24]

i. Preparation of Sample Solutions. For all measurements sample solutions were prepared as follows: Solid polymer samples (recovered by a freeze-drying technique) were dissolved into pure water or D_2O (for NMR measurements) at 90 °C with vigorous stirring for 15 min. After cooling the solutions to room temperature, a predetermined amount of NaCl was added to the polymer solutions to adjust ionic strength.

Table 1. Molecular Weights and Hydrodynamic Radii of the C_6-, C_{12}-, and C_{18}-Carrying Polymers

hydrophobic comonomer	hydrophobe content (mol %)	M_w[a] ($\times 10^4$)	M_w/M_n[a]	R_h[b] (nm)
C_6MAm	0	1.1	2.1	7.3
	5	0.9	2.5	5.7
	10	0.8	2.6	4.4, 54
	20	1.8	3.3	12
	30	2.1	4.2	7.3
	40	2.2	4.0	5.9
	50	2.2	3.7	4.8
	60	2.2	3.1	4.0
	70	1.8	2.3	3.8
	80	2.0	2.2	8.1
C_{12}MAm	10	2.8	2.2	7.1
	20	3.1	2.2	4.9
	30	2.6	2.4	3.9
	40	3.0	2.2	4.0
	50	1.5	1.9	4.3
	55	1.5	2.1	5.7
	60	1.9	1.8	8.1
C_{18}MAm	5	1.5	2.9	9.8
	10	1.3	3.3	7.1
	20	0.8	2.1	6.7
	25	0.9	2.5	16
	30	1.5	2.2	6−10, 48
	35	1.0	2.2	15
	40	0.9	1.5	31

[a] Determined by GPC using methanol containing 0.2 M $LiClO_4$ as an eluent at 40 °C. [b] Determined by QELS in 0.05 M NaCl aqueous solutions at 25 °C.

Results

Characteristics of the Polymers. We reported previously that the copolymerization of AMPS and C_{12}MAm[36] and also the copolymerization of AMPS and 1-NpMAm[27] were characterized as "ideal copolymerization" systems, resulting in copolymer compositions equal to monomer feed compositions and completely random distributions of the two monomer units along the polymer chain. In the case of the terpolymerization of AMPS, C_6MAm or C_{18}MAm, and 1-NpMAm, we confirmed that the composition in the terpolymer is virtually the same as that in the monomer feed as in the case of the terpolymer of AMPS, C_{12}MAm, and 1-NpMAm synthesized previously.[22] Therefore, the distributions of the monomer units along the polymer chain for the terpolymers are essentially random.

In Table 1 are listed weight-average molecular weights (M_w) estimated by GPC in methanol containing 0.2 M $LiClO_4$ for the three terpolymers with varying hydrophobe contents. In our earlier work on AMPS-C_{12}MAm copolymers, we confirmed that M_w values estimated by GPC in methanol containing 0.2 M $LiClO_4$ using poly(ethylene oxide) standards for calibration are a rough measure of "real" M_w determined by SLS.[24] Thus, we performed GPC measurements to roughly assess M_w. As can be seen from Table 1, M_w values for all the polymers are of the same order of magnitude, $(0.8−2.2) \times 10^4$, $(1.1−3.1) \times 10^4$, and $(0.8−1.5) \times 10^4$ for the C_6MAm, C_{12}MAm, and C_{18}MAm containing terpolymers, respectively. Dry samples of these terpolymers are soluble in water, yielding optically clear solutions, up to the alkylmethacrylamide contents of 80, 60, and 40 mol % for the C_6MAm, C_{12}MAm, and C_{18}MAm containing terpolymers, respectively. When the alkylmethacrylamide contents in the respective polymers

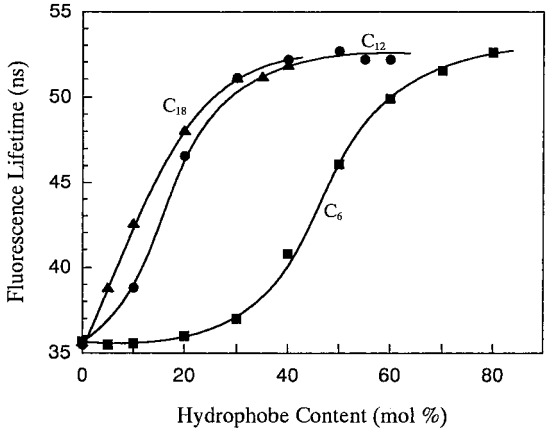

Figure 1. Fluorescence lifetimes for naphthalene labels in the C_6-, C_{12}-, and C_{18}-carrying polymers plotted as a function of the hydrophobe content: Polymer concentration: 1 g/L in a 0.05 M NaCl aqueous solution.

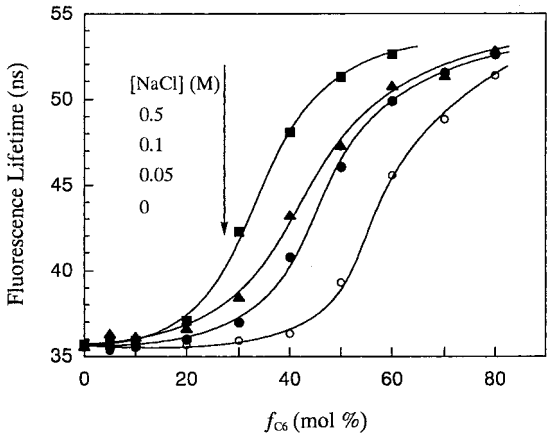

Figure 2. Plots of the fluorescence lifetimes for naphthalene labels in the C_6-carrying polymers as a function of f_{C6} at varying concentrations of added NaCl. Polymer concentration: 1 g/L.

exceed these levels, polymers become insoluble in water. Therefore, in this study, we employed polymers with hydrophobe contents lower than these solubility limits.

Fluorescence Lifetime. The polarity of microenvironments around naphthalene labels is known to be reflected in their fluorescence lifetimes; the lifetime is longer in less polar media.[37] When the hydrophobe content is sufficiently high, polymer-bound hydrophobes aggregate into a microdomain in which naphthalene labels may be entrapped. On the other hand, if hydrophobe contents are low, naphthalene labels would be exposed to the aqueous phase.

Fluorescence lifetime measurements for the naphthalene-labeled polymers were performed in 0.05 M NaCl aqueous solution at 25 °C. All the fluorescence decay data for polymers possessing C_6, C_{12}, and C_{18} alkyl chains (Chart 1) were best-fitted to a single-exponential function with χ^2 ranging from 1.0 to 1.3 independent of the hydrophobe content. Fluorescence lifetimes are plotted in Figure 1 against the hydrophobe content for the three polymers with different alkyl chain lengths. When the hydrophobe content is zero (i.e., naphthalene-labeled polyAMPS), the fluorescence lifetime is 36 ns. However, the lifetime increases up to ca. 53 ns when the hydrophobe contents are sufficiently high for all the polymers. These observations indicate that, with increasing hydrophobe content, the formation of hydrophobic domains proceeds, and naphthalene labels are incorporated in hydrophobic domains. Hence, the fluorescence lifetime provides information about the formation of hydrophobic domains. The longest lifetime observed (ca. 53 ns) thus reflects a situation where the labels are completely incorporated in hydrophobic domains formed by the polymer-bound alkyl chains.

As can be seen from Figure 1, the lifetime increases significantly in a relatively narrow range of the hydrophobe contents in the polymer depending on the length of the alkyl chain. In the case of the C_6 alkyl chain, the fluorescence lifetimes are practically the same as that of polyAMPS-bound naphthalene up to a C_6MAm content (f_{C6}) of ca. 20 mol %, suggesting all naphthalene labels are exposed to the aqueous phase. The lifetime starts to increase significantly near $f_{C6} \approx 30$ mol % and continues to increase with increasing f_{C6} up to 80 mol % although the increase slows down at $f_{C6} > 60$ mol %, exhibiting a tendency for saturation near a lifetime of ca. 53 ns. On the other hand, in the cases of the C_{12} and C_{18} chains, the lifetime increases to a saturated level at much lower hydrophobe contents than in the case of the C_6 chain. In our earlier work on AMPS-C_{12}MAm copolymers, we confirmed that the formation of hydrophobic domains could be monitored through the micropolarity reported by fluorescence labels.[22] Thus, we can interpret the results in Figure 1 as indicating that the self-association of polymer-bound C_6 chains starts to occur at a much higher hydrophobe content than in the cases of the C_{12} and C_{18} chains. It should be noted that the saturated value of the lifetime is constant at ca. 53 ns regardless of the length of the alkyl chain.

The sigmoidal curve observed for the C_6 polymers suggests that the hydrophobic association occurs in a cooperative manner. Namely, once hydrophobic association starts to occur at a certain hydrophobe content, polymer-bound hydrophobes associate more favorably, leading to a large increase in the formation of hydrophobic domains in a relatively narrow range of hydrophobe contents.

Associations of polyelectrolyte-bound hydrophobes occur competing with electrostatic repulsion. Therefore, added salt enhances the hydrophobic association by shielding electrostatic repulsive interactions. Fluorescence lifetimes for the C_6 polymers at varying concentrations of added salt are presented in Figure 2. With increasing ionic strength, the hydrophobe content at which the lifetime starts to increase shifts toward lower f_{C6}. At $f_{C6} < 20$ mol %, the effect of added salt on the fluorescence lifetime is small because the numbers of the C_6 chains per polymer are not enough to form hydrophobic domains even though electrostatic repulsions are shielded by added salt. On the other hand, when f_{C6} is sufficiently high (i.e., $f_{C6} > 70$ mol %), the effect of added salt on the fluorescence lifetime is small because the hydrophobic association prevails over electrostatic repulsion even without salt added due to a large enough number of hydrophobes relative to the number of charge in the polymer. A most pronounced salt effect was observed in the regime $40 < f_{C6} < 50$ mol %. For example, the lifetime for $f_{C6} = 40$ mol % is ca. 36 ns in pure water, but it increases to ca. 48 ns in a 0.5 M NaCl aqueous solution. These observations suggest that the AMPS-C_6MAm copolymers may find an application as a salt-responsive water-soluble polymer because they adopt an open chain conformation in pure water but collapse into a compact conformation

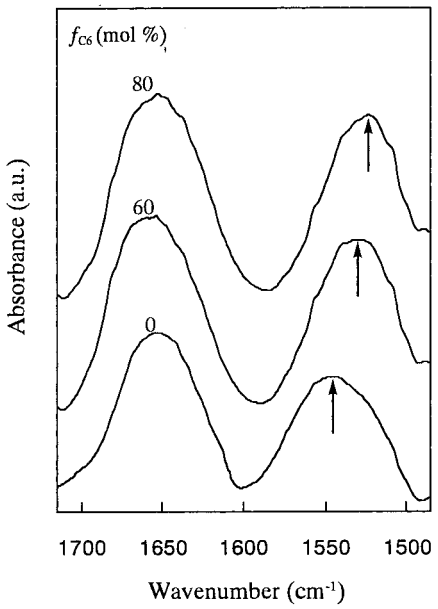

Figure 3. FT-IR spectra for the C_6-carrying polymers with f_{C6} = 0, 60, and 80 mol % measured as KBr pellets. Arrows indicate the amide II band.

(see later subsection) accompanied by the formation of hydrophobic domains in saltwater. It is to be noted here that the copolymers with f_{C6} = 70 and 80 mol % were found to be insoluble in 0.5 M NaCl aqueous solutions because of a salting-out effect.

FT-IR. Figure 3 shows an example of FT-IR spectra for the C_6 polymers with f_{C6} = 60 and 80 mol % compared in the range 1500−1700 cm^{-1}. An IR spectrum for naphthalene-labeled polyAMPS (i.e., f_{C6} = 0 mol %) is also presented as a reference in Figure 3. For FT-IR measurements, we used solid polymer samples recovered from ca. 1 g/L aqueous solutions of the polymers by a freeze-drying technique. All the polymers show two characteristic IR absorption bands in this wavenumber region due to the amide bond, the peaks at higher and lower wavenumbers attributable to amide C═O stretching vibration (amide I band) and amide N−H deformation (amide II band), respectively. An observation to be noted is that the amide II band for the C_6 polymers shifts toward lower wavenumbers comparing to that for the reference polymer. This lower-wavenumber shift is ascribable to the hydrogen bonding of amide spacer bonds.

As we discussed previously,[17] micellar structures formed from associations of polyelectrolyte-bound hydrophobes in aqueous solutions are retained, if not perfectly, in freeze-dried solid samples. Hydrophobic domains in the micellar structures are microscopically phase-separated from the water phase and sustained in water by hydrated polyelectrolyte segments around the hydrophobic domains. This microphase-separated structure should remain intact when aqueous solutions are frozen. When the frozen solution is subjected to freeze-drying, water molecules in the bulk phase and in the hydration layer are removed, leaving a polymer solid phase behind with the microphase structures remaining as such. Therefore, it is reasonable to consider that the hydrogen bonds detected by FT-IR (Figure 3) are those existing in association structures in aqueous solutions.

We measured IR spectra on the C_6 polymers of varying f_{C6}, and the wavenumbers of the amide II band

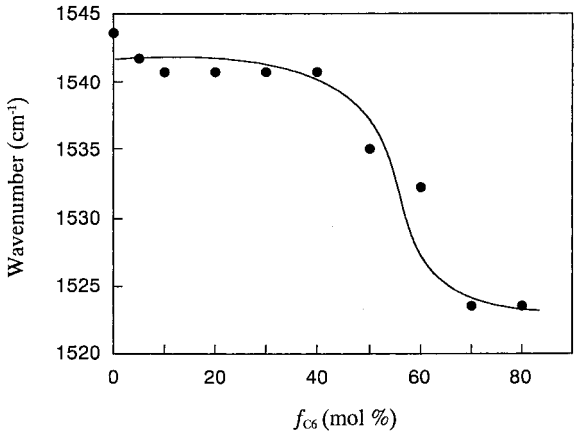

Figure 4. Plot of the wavenumber of the amide II band for the C_6 polymers as a function of f_{C6}.

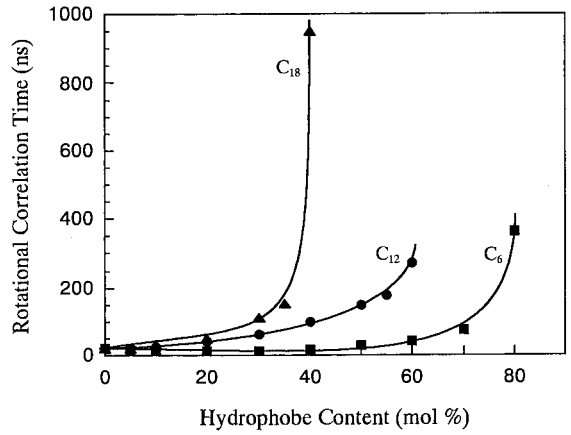

Figure 5. Rotational correlation times for the C_6-, C_{12}-, and C_{18}-carrying polymers determined by fluorescence depolarization plotted as a function of the hydrophobe content. The depolarization experiments were performed with 1 g/L polymer solutions containing 0.05 M NaCl at 25 °C. The data for the C_{12} copolymers are cited from ref 23.

are plotted in Figure 4 as a function of f_{C6}. The wavenumbers are practically constant at f_{C6} < 40 mol %. However, the wavenumber commences to decrease near $f_{C6} \approx$ 50 mol % with increasing f_{C6} and eventually saturates in the range 70 < f_{C6} < 80 mol %, exhibiting a wavenumber shift of ca. 20 cm^{-1} compared to the amide II band of the reference polymer of f_{C6} = 0 mol %. This tendency fairly agrees with the tendency of the fluorescence lifetime shown in Figure 1, thus suggesting that hydrogen bonding is more favorably formed between the spacer amide bonds when the C_6 chains form hydrophobic domains. Hence, we can monitor the formation of hydrophobic domains by IR spectroscopy focusing on the amide II band.

Fluorescence Depolarization. Fluorescence depolarization of naphthalene labels covalently linked to a polymer chain is a useful tool for studies of dynamic properties of the polymer chain.[38,39] Previously, we demonstrated that fluorescence depolarization of naphthalene labels on hydrophobically modified polyelectrolytes provided information on the formation of hydrophobic domains due to the fact that local motions of naphthalene labels are restricted when the labels are incorporated in the hydrophobic domains.[23]

In Figure 5, rotational correlation times (τ_ϕ) for naphthalene labels in the C_6, C_{12}, and C_{18} polymers, calculated from anisotropy (r) values using eq 2, are

plotted as a function of the hydrophobe content. In general, not only local motions of a fluorescence label within a polymer environment but also motions of the whole polymer molecule would contribute to the fluorescence depolarization. The rotational correlation time for a rigid sphere (τ_s) of the radius of R is given by

$$\tau_s = 4\pi R^3 \eta / k_B T \tag{8}$$

In the case of the C_6 polymer, the hydrodynamic radius (R_h) for $f_{C6} = 80$ mol % was observed to be 8.1 nm by QELS (see later subsection). Assuming this polymer as a rigid sphere with a radius of 8 nm, the rotational correlation time for the polymer molecule may be roughly estimated from eq 8 to be 1.4 μs, which is much longer than a value of τ_ϕ (360 ns) observed from the fluorescence depolarization of naphthalene labels on the C_6 polymer (Figure 5). From similar estimations of the rotational correlation times for the other polymers as compared to the observed τ_ϕ values, we concluded that the τ_ϕ values observed for naphthalene labels reflect essentially the rotational motions of the label itself in polymer environments.

In the case of the C_6 polymer, τ_ϕ values are practically constant at $f_{C6} < 50$ mol %, and the value starts to increase near $f_{C6} \approx 60$ mol % with increasing f_{C6}, followed by a sharp increase between $f_{C6} = 70$ and 80 mol %. This tendency is in contrast to the tendency observed for the fluorescence lifetime (Figure 1). In the region $60 < f_{C6} < 80$ mol %, the τ_ϕ value increases significantly, whereas the fluorescence lifetime exhibits a saturation tendency, that is, when f_{C6} is increased from 60 to 80 mol %, the fluorescence lifetime increases only by ca. 3 ns, whereas the τ_ϕ value greatly increases from ca. 40 to 360 ns. This indicates that at $f_{C6} \approx 60$ mol % the labels are incorporated into hydrophobic domains formed by C_6 chains and experience a hydrophobic microenvironment, but the labels can rotate quite freely within the hydrophobic domain. With an increase in f_{C6} beyond 60 mol %, motions of the labels become more restricted although the micropolarity around the labels has already reached a saturated level.

In the cases of the C_{12} and C_{18} polymers, the τ_ϕ values increase gradually first as the hydrophobe contents are increased and then start to increase sharply at $f_{C12} \approx 55$ and $f_{C18} \approx 35$ mol %, respectively. The lifetimes of naphthalene fluorescence for these two polymers reach a saturated level of ca. 53 ns at hydrophobe contents near 30 mol % (Figure 1), but there is a large difference in the τ_ϕ values between the C_{12} and C_{18} polymers at higher hydrophobe contents. In the case of the C_{18} polymer, the τ_ϕ value jumps up to ca. 950 ns at $f_{C18} = 40$ mol %, while the τ_ϕ value for the C_{12} polymer at the same hydrophobe content is only ca. 100 ns.

Results in Figure 5, taken together with results in Figure 1, led us to conclude as follows: The C_6, C_{12}, and C_{18} alkyl chains undergo self-association to form hydrophobic domains when their contents in the polymers exceed a certain level that is dependent on the length of the alkyl chain. The size of the hydrophobic domain grows with increasing hydrophobe content to an extent where naphthalene labels are completely entrapped. Even after the labels are completely incorporated in hydrophobic domains, thus reporting a saturated micropolarity in their fluorescence lifetimes, the rigidity of the hydrophobic domain greatly increases with further increasing hydrophobe content, hence the labels reporting a large increase in their motional restriction. The rigidity or tightness of the hydrophobic domain depends strongly on the length of the alkyl chain. As the number of carbon atoms in an alkyl chain is increased, the tightness of hydrophobic domains increases greatly. Thus, the largest extent of the motional restriction of the naphthalene label is observed for the C_{18} chains whereas the smallest extent was observed for the C_6 chains. These results suggest that the rigidity of hydrophobic domain is related to the dynamic motion of each alkyl chain within the domain; i.e., shorter chains can move more freely in the domain.

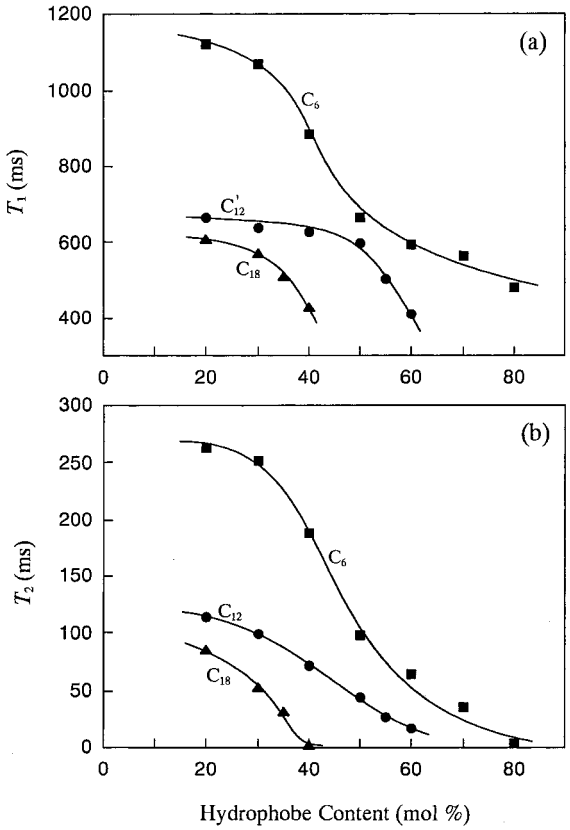

Figure 6. Plots of T_1 (a) and T_2 (b) for methyl protons in the polymer-bound C_6, C_{12}, and C_{18} alkyl chains as a function of the hydrophobe content measured in D_2O containing 0.05 M NaCl at 30 °C. The data for the C_{12} polymers are cited from ref 23.

^{1}H NMR Relaxation Times. ^{1}H NMR relaxation techniques provide a useful tool to study local motions of polymer chains.[29−31] We performed ^{1}H NMR relaxation time measurements on the C_6, C_{12}, and C_{18} polymers in D_2O containing 0.05 M NaCl to obtain information about changes in the dynamic motion of the alkyl chains upon hydrophobic association. For the calculation of the spin−lattice relaxation time (T_1) and the spin−spin relaxation time (T_2), we chose the methyl proton peak in the C_6, C_{12}, and C_{18} alkyl chains because the methyl protons in these alkyl chains give an isolated peak at ca. 0.9 ppm, whereas the methylene proton peak in the alkyl chains (at ca. 1.3 ppm) overlaps with peaks due to the methyl protons in the AMPS unit and the methyl and methylene protons in the main chain.[23] In Figure 6, T_1 and T_2 values are plotted against the hydrophobe content. (Resonance peaks due to the methyl protons for 10 mol % hydrophobe content were so small that we were unable to determine T_1 and T_2 values.) The spin−lattice relaxation occurs most ef-

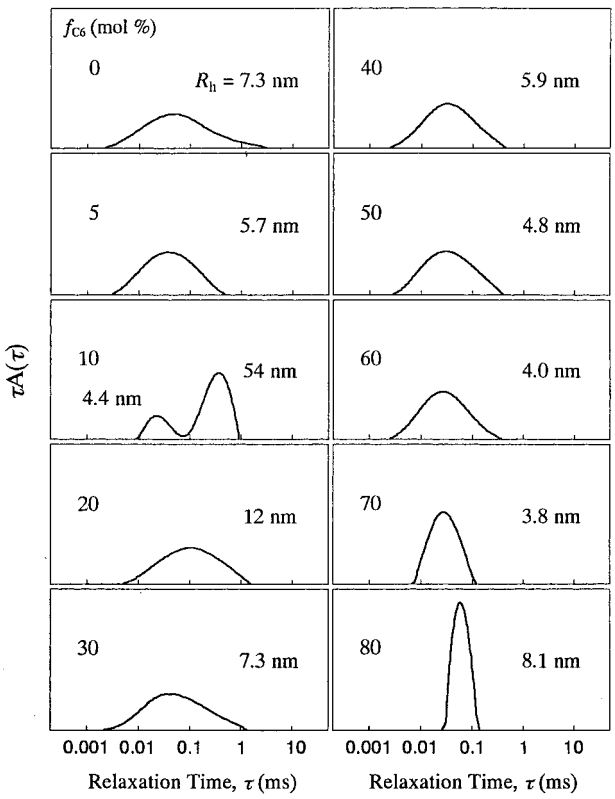

Figure 7. Relaxation time distributions in QELS observed at $\theta = 90°$ for the C_6 polymers at 25 °C. Polymer concentration: 1 g/L in a 0.05 M NaCl aqueous solution.

ficiently through molecular motions whose frequency is comparable to the NMR frequency.[40] Therefore, T_1 decreases concurrently with T_2 as the molecular motion decreases. In the case of the C_6 chain, both T_1 and T_2 values decrease significantly in the range $30 < f_{C6} < 60$ mol %. This tendency is similar to that observed for the fluorescence lifetime of naphthalene labels (Figure 1) but different from the tendency observed for the fluorescence depolarization (Figure 5). In the cases of the C_{12} and C_{18} chains, both T_1 and T_2 values are already decreased greatly at their content of 20 mol %, indicating that hydrophobic domains are formed at lower hydrophobe contents than in the case of the C_6 chain, consistent with the results in Figure 1. The T_1 values for the C_{12} and C_{18} chains show a tendency to decrease more significantly with increasing their contents near 50 and 30 mol %, respectively. This tendency is somewhat similar to the tendency observed for the fluorescence depolarization (Figure 5). These observations indicate that the motional freedom of the terminal methyl group in alkyl chains depends strongly on the length of the alkyl chain when they form hydrophobic domains.

QELS. Distributions of the relaxation times (τ) in QELS for the C_6 polymers with varying f_{C6} in 0.05 M NaCl aqueous solutions observed at a scattering angle of 90° are presented in Figure 7. The relaxation time distributions were also measured at varying scattering angles (50°−130°), and the relaxation rate (Γ) (i.e., the reciprocal of the relaxation time) at each peak top was plotted against the square of scattering vector (q^2), yielding a straight line passing through the origin (data not shown). From the translational diffusion coefficient (D) determined from the slope of the $\Gamma - q^2$ plot, R_h was calculated using eq 7. Values of R_h thus estimated are listed in Table 1. The distribution is unimodal for $f_{C6} = 5$ mol %, but it becomes bimodal when f_{C6} is increased to 10 mol %. In our earlier work on AMPS-C_{12}MAm copolymers,[25] we observed that at $f_{C12} < 10$ mol % QELS relaxation time distributions were bimodal with a fast relaxation mode attributable to unimers (a single molecular state) and a slow mode to multipolymer aggregates. The slow mode peak in the bimodal distribution observed for the C_6 polymer with $f_{C6} = 10$ mol % (Figure 7) is an indication of the interpolymer association of C_6 chains yielding multipolymer aggregates with $R_h = 54$ nm. The fast mode peak corresponding to $R_h = 4.4$ nm is presumably due to unimers. When f_{C6} is increased to 20 mol %, the distribution becomes unimodal, but R_h is significantly larger than those for $f_{C6} = 0$ and 5 mol % (Table 1), suggesting that the polymer undergoes interpolymer association as in the case of the AMPS-C_{12}MAm copolymers of $f_{C12} < 10$ mol %.[25] With increasing f_{C6} in the range $20 \le f_{C6} \le 70$ mol %, R_h decreases from 12 to 3.8 nm. This decrease in R_h in this f_{C6} range indicates that hydrophobic associations of C_6 chains occur progressively in a intrapolymer fashion, leading to the formation of unimolecular micelles as in the case of the AMPS-C_{12}MAm copolymers with hydrophobe contents in the range $20 < f_{C12} < 50$ mol %.[23] However, when f_{C6} is further increased to 80 mol %, R_h increases rather abruptly to 8.1 nm. A similar tendency was also observed for the AMPS-C_{12}MAm copolymers.[23] When f_{C12} in the AMPS-C_{12}MAm copolymer was increased to 55 mol % or higher, R_h increased abruptly, indicating the formation of multipolymer aggregates.[23] These multipolymer aggregates formed at $f_{C12} \ge 55$ mol % are markedly different from those observed at $f_{C12} < 10$ mol % in that the relaxation distributions for $f_{C12} \ge 55$ mol % are unimodal with a narrow width, whereas the distributions for $f_{C12} < 10$ mol % are bimodal.[23] The same unimodal distribution with a narrow width observed for the C_6 polymer with $f_{C6} = 80$ mol % (Figure 7) corresponds to the same type of multipolymer aggregates observed for the AMPS-C_{12}MAm copolymers with $f_{C12} \ge 55$ mol %.

Relaxation time distributions for the C_{18} polymers with varying f_{C18} in 0.05 M NaCl aqueous solutions observed at a scattering angle of 90° are presented in Figure 8. Values of R_h estimated from $\Gamma - q^2$ plots are listed in Table 1. In contrast to the case of the C_6 polymer, R_h increases from 7.3 to 9.8 nm when f_{C18} is increased from 0 to 5 mol % and then decreases to 6.7 nm as f_{C18} is further increased to 20 mol %. The larger R_h observed for $f_{C18} = 5$ mol % may be due to the same type of the intermolecularly associated polymer chains observed for the C_6 and C_{12} polymers when hydrophobe contents are low. In the case of the C_{18} polymers, a progressive decrease in R_h is observed in the range $5 < f_{C18} < 20$ mol %, followed by an increase in R_h as f_{C18} is further increased. This suggests that an increase in f_{C18} in this f_{C18} region leads to an increase in the tendency for intrapolymer association of the C_{18} chains whereas a further increase in f_{C18} leads to an inclination for interpolymer associations to form multipolymer aggregates. At $f_{C18} = 25$ mol %, the distribution appears to be bimodal with a major peak apparently due to multipolymer aggregates with $R_h = 16$ nm and a small shoulder on the longer relaxation time side corresponding to larger aggregates. When f_{C18} is increased to 30 mol %, the distribution remains bimodal but with a large peak of a much longer relaxation time correspond-

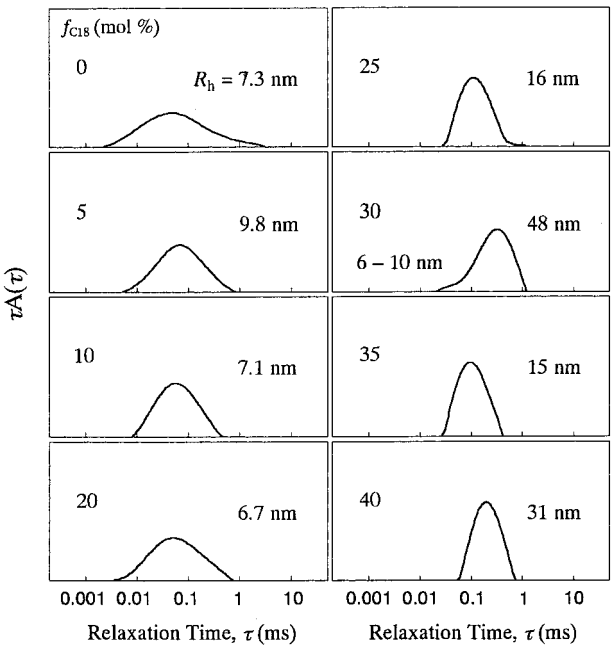

Figure 8. Relaxation time distributions in QELS observed at $\theta = 90°$ for the C_{18} polymers at 25 °C. Polymer concentration: 1 g/L in a 0.05 M NaCl aqueous solution.

ing to multipolymer aggregates with $R_h = 48$ nm and a small shoulder on the side of shorter relaxation times apparently due to unimers or small interpolymer aggregates. At present, it is not well understood why the relaxation time distributions at $f_{C18} = 25$ and 30 mol % are so different and the polymer with $f_{C18} = 30$ mol % shows the presence of considerably larger aggregates as a major component. The structure of the larger aggregates remains an open question. This type of association behavior is unique to the C_{18} alkyl chain because no such larger aggregates were observed for the C_6 and C_{12} polymers. As f_{C18} is further increased to 35 mol % or more, the distributions become unimodal and narrower, suggesting the formation of the same type of multipolymer aggregates as that for the AMPS-C_{12}MAm copolymers with $f_{C12} \geq 55$ mol %.[23]

Discussion

The polymers with C_6, C_{12}, and C_{18} alkyl chains exhibit the smallest R_h values of 3.8, 3.9, and 6.7 nm at hydrophobe contents of 70, 30, and 20 mol %, respectively (Table 1). At these hydrophobe contents, polymer aggregates formed are likely to be unimolecular micelles or multipolymer micelles formed from a small number of polymer chains. We attempted to estimate the compactness of these micelles by comparing apparent M_w and R_h values for the micelles. We determined M_w by SLS for the C_6, C_{12}, and C_{18} polymers with the smallest R_h to be 6.5×10^4, 5.3×10^4, and 11.5×10^4, respectively. Since we found it difficult to measure SLS for polymer solutions in 0.05 M NaCl, we chose to use polymer solutions in 0.2 M NaCl. In a separate QELS experiment, we confirmed that in 0.2 M NaCl the polymers form practically the same type of aggregates as that formed in 0.05 M NaCl. From these M_w and R_h values, apparent densities (i.e., mass/hydrodynamic volume) of the polymer aggregates are calculated to be 0.47, 0.36, and 0.15 g/cm^3 for the polymers of $f_{C6} = 70$ mol %, $f_{C12} = 30$ mol %, and $f_{C18} = 20$ mol %, respectively. These apparently low densities are presumably due to the fact that the hydrodynamic volume of the polymer aggregate is mainly determined by the size of extended hydrophilic loops of AMPS segments surrounding hydrophobic microdomains. Because the size of the hydrophilic loop increases with the AMPS content, the apparent density decreases in the order of ($f_{C6} = 70$ mol %) > ($f_{C12} = 30$ mol %) > ($f_{C18} = 20$ mol %).

Association structures depend on protocol for the preparation of aqueous solutions of the polymers.[24] In the present work, polymers were purified by reprecipitation from methanol solutions into excess diethyl ether, followed by dialysis of aqueous polymer solutions against pure water. Solid polymer samples were recovered from the dialyzed aqueous solutions by freeze-drying. Our previous study revealed that there existed multipolymer micelles in the freeze-dried samples that had been formed by hydrophobic associations of entangled polymer chains during the purification procedure.[24] When the solid polymer samples are added to pure water at room temperature, the already existing multipolymer micelles are simply redissolved in water as such. However, if the aqueous solution was heated to 90 °C, followed by the addition of a predetermined amount of NaCl to adjust ionic strength of the solution, the chain entanglement could be eliminated, forming unimolecular micelles if the polymers has a strong tendency, as its intrinsic nature, for preferential intrapolymer association.[24] In the present study, we employed these procedures to prepare polymer solutions in 0.05 or 0.2 M NaCl. Thus, it is expected that virtually unimolecular micelles were obtained for polymers having a strong tendency for intrapolymer association.[24]

In our earlier work on the C_{12} polymers, we observed that M_w values for unimers determined by SLS in 0.2 M NaCl were 2−4 times larger than those estimated by GPC in methanol calibrated with poly(ethylene oxide).[24] Thus, the M_w values presently determined by SLS for the 70 mol % C_6 and 30 mol % C_{12} polymers (ca. 4 and 2 times larger than those estimated by GPC, respectively) suggest that the polymer aggregates are mostly unimolecular micelles. However, micelles formed from the C_6 and C_{12} polymers with higher hydrophobe contents (i.e., $f_{C6} > 70$ mol % and $f_{C12} > 50$ mol %) are multipolymer micelles probably because chain entanglements could not be eliminated completely during the process of the preparation of polymer solutions. In the case of the 20 mol % C_{18} polymer, however, the M_w value by SLS is ca. 14 times larger than that estimated by GPC, suggesting that the polymer aggregates are not unimolecular but multipolymer micelles. These observations indicate that the tendency for intrapolymer hydrophobic association is much smaller for the C_{18} alkyl chain than the C_6 and C_{12} chains. At present, it is not understood whether this is due to an intrinsic nature of the longer alkyl chain or an increased difficulty of chain disentanglement during the process of polymer solution preparation.

Results of the present study, together with results of our earlier work on AMPS-C_{12}MAm copolymers, indicate that intrapolymer associations occur dominantly for the C_6 and C_{12} polymers in the range $30 < f_{C6} < 70$ mol % and $10 < f_{C12} < 50$ mol %. A similar tendency was observed for the C_{18} polymers in the range $5 < f_{C18} < 20$ mol % although polymer aggregates formed in this range were not purely unimolecular. When hydrophobe contents are lower than these ranges, a significant extent of interpolymer associations occur concurrently,

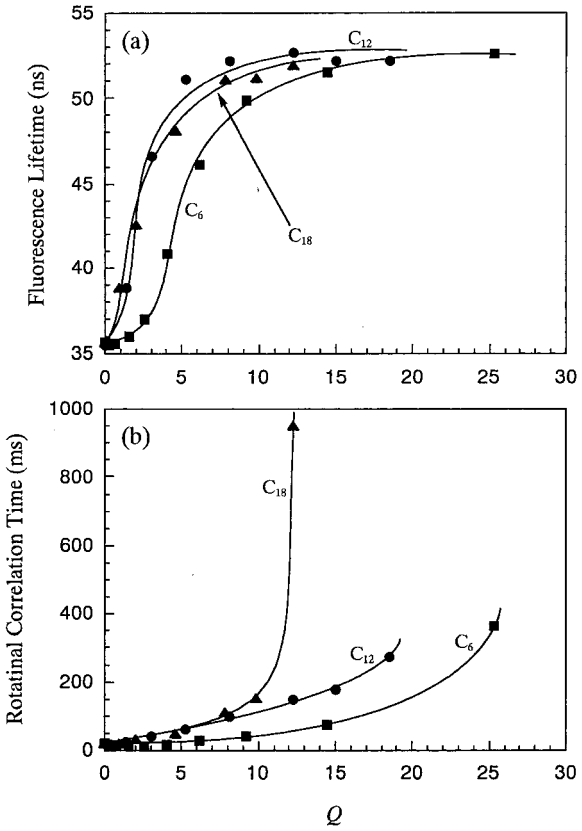

Figure 9. Plots of the fluorescence lifetime (a) and rotational correlation time (b) for naphthalene labels in the C_6-, C_{12}-, and C_{18}-carrying polymers plotted as a function of the hydrophobe/charge ratio Q.

yielding larger aggregates, and QELS relaxation times exhibit bimodal distributions attributed to multipolymer aggregates and coexisting unimers. On the other hand, when hydrophobe contents are higher than these ranges, multipolymer aggregates are formed predominantly, and QELS relaxation times exhibit unimodal distributions with a narrow width. Lower and upper limits for the preferential intrapolymer association to occur shift toward lower hydrophobe contents, and the width between the lower and upper limits becomes narrower as the length of the alkyl chain increases.

To compare the "effectiveness" of the C_6, C_{12}, and C_{18} alkyl chains per carbon atom for hydrophobic self-association, we define a parameter Q which represents a hydrophobe/charge ratio in a polymer chain as

$$Q = \frac{Nf_{CN}}{99 - f_{CN}} \tag{9}$$

where N is the number of carbon atoms in an alkyl chain, and f_{CN} is the mole percent content of a methacrylamide substituted with an alkyl chain with N carbon atoms. The solubility limits of 80, 60, and 40 mol % alkylmethacrylamide contents for the respective C_6, C_{12}, and C_{18} polymers correspond to $Q \approx 25$, 18, and 12, respectively. Thus, the maximum hydrophobe/charge ratio of the polymer soluble in water decreases significantly with increasing length of the alkyl chain. In other words, with a shorter alkyl chain as a hydrophobe, one can incorporate more carbon atoms into a polymer keeping the polymer water-soluble.

In Figure 9, the fluorescence lifetimes and rotational correlation times for fluorescence depolarization are plotted as a function of Q. As can be seen from Figure 9a, the lifetime plots for the C_{12} and C_{18} polymers follow similar lines, indicating that there is no significant difference in the effectiveness of the C_{12} and C_{18} alkyl chains per carbon atom for the formation of hydrophobic domains. The C_{12} and C_{18} chains can form hydrophobic domains even at a low level of Q (i.e., $Q \approx 1$), and the domain formation further proceeds with increasing Q, reaching a saturated level near $Q \approx 10$. In the case of the C_6 chains, by contrast, the domain formation is not significant at $Q < 3$, but it proceeds with increasing Q over the range of $3 < Q < 15$. The formation of hydrophobic domains for the C_6 chains is more gradual than in the cases of the C_{12} and C_{18} chains. These findings indicate that the C_6 alkyl chains are less effective for the self-association than the C_{12} and C_{18} chains per carbon atom. In other words, with C_6 chains, one needs more carbon atoms to incorporate into a polymer than with C_{12} and C_{18} chains to attain the same extent of the hydrophobic domain formation.

Although the effectiveness of the C_{12} and C_{18} chains in hydrophobic associations looks similar when monitored by the fluorescence lifetime of naphthalene labels, the extent of the motional restriction imposed on the labels in the hydrophobic domains monitored by fluorescence depolarization is quite different at $Q > 10$ (Figure 9b). At $Q < 8$, hydrophobic domains formed by the C_{12} and C_{18} chains are similar in the extent of the motional restriction of the labels, but at $Q > 10$, the C_{18} domains impose much more restriction on the labels than do the C_{12} domains. In the case of the C_6 chains, the extent of the motional restriction increases gradually with increasing Q over the whole range of Q shown in Figure 9b and is much less than the cases of the C_{12} and C_{18} chains. A similar conclusion can be drawn from the dependence of ^{1}H NMR relaxation times on Q (plots not shown).

Conclusions

The self-association properties in water of AMPS copolymers with methacrylamides N-substituted with a C_6 or C_{18} alkyl chain were investigated by fluorescence decay and depolarization, FT-IR, ^{1}H NMR relaxation, and QELS techniques, focusing on the effect of the length of the alkyl chain on the hydrophobic self-association behavior. Experimental results were compared with those of the same type of AMPS copolymers carrying C_{12} alkyl chains in our earlier work. The polymer-linked C_6 chains commence to undergo self-association at a much higher hydrophobe content than in the cases of the C_{12} and C_{18} chains. The polymer-bound C_6 and C_{12} alkyl chains undergo predominantly intrapolymer self-associations when the hydrophobe contents are in the range of 30−70 and 10−50 mol %, respectively. In the case of the polymer-bound C_{18} chains, there is a similar tendency for intrapolymer association when the hydrophobe contents are in the range of 5−20 mol %, but polymer aggregates formed are not completely unimolecular. If the hydrophobe contents are either lower or higher than these limits, intermolecularly associated structures with larger hydrodynamic volumes are formed. It was found that the dynamic properties of hydrophobic domains formed by alkyl chains with different lengths are considerably different. Although micropolarity experienced by naphthalene labels incorporated in the hydrophobic domain is the same, motional restrictions imposed on the labels

are more pronounced when the domains are formed from longer alkyl chains. The same tendency of restricted motions of the alkyl chains was indicated by ^{1}H NMR relaxation times. The effectiveness of the methylene and methyl residues in the polymer-bound C_6, C_{12}, and C_{18} chains to self-associate was compared in terms of a parameter representing the hydrophobe/charge ratio. The CH_2 and CH_3 residues in the C_6 chain are much less effective than those in the C_{12} and C_{18} chains in hydrophobic associations when compared at the same hydrophobe/charge ratio in a polymer chain, whereas there is no significant difference between those in the C_{12} and C_{18} chains.

Acknowledgment. This work was supported in part by a Grant-in-Aid for Scientific Research No. 10450354 from the Ministry of Education, Science, Sports and Culture, Japan, and in part by Shorai Foundation for Science and Technology.

References and Notes

(1) *Principles of Polymer Science and Technology in Cosmetics and Personal Care*; Goddard, E. D., Gruber, J. V., Eds.; Marcel Dekker: New York, 1999.
(2) McCormick, C. L.; Bock, J.; Schulz, D. N. *Encyclopedia of Polymer Science and Engineering*; John Wiley: New York, 1989; Vol. 17, p 730.
(3) Bock, J.; Varadaraj, R.; Schulz, D. N.; Maurer, J. J. In *Macromolecular Complexes in Chemistry and Biology*; Dubin, P., Bock, J., Davies, R. M., Schulz, D. N., Thies, C., Eds.; Springer-Verlag: Berlin, 1994; p 33.
(4) *Polymers as Rheology Modifiers*; Schulz, D. N., Glass, J. E., Eds.; Advances in Chemistry Series 462; American Chemical Society: Washington, DC, 1991.
(5) *Hydrophilic Polymer, Performance with Environmental Acceptability*; Glass, J. E., Ed.; Advances in Chemistry Series 248; American Chemical Society: Washington, DC, 1996.
(6) Valint, P. L., Jr.; Bock, J.; Schulz, D. N. In *Polymers in Aqueous Media: Performance through Association*; Glass, J. E., Ed.; Advances in Chemistry Series 223; American Chemical Society: Washington, DC, 1989; p 399.
(7) Kamioka, K.; Webber, S. E.; Morishima, Y. *Macromolecules* **1988**, *21*, 972.
(8) Morishima, Y.; Lim, H. S.; Nozakura, S.; Strutevant, J. L. *Macromolecules* **1989**, *22*, 1148.
(9) McCormick, C. L.; Chang, Y. *Macromolecules* **1994**, *27*, 2151.
(10) Prochazka, K.; Kiserow, D.; Ramireddy, C.; Tuzar, Z.; Munk, P.; Webber, S. E. *Macromolecules* **1992**, *25*, 454.
(11) McCormick, C. L.; Salazar, L. C. *Polymer* **1992**, *33*, 4617.
(12) Chang, Y.; McCormick, C. L. *Macromolecules* **1993**, *26*, 6121.
(13) Morishima, Y. *Trends Polym. Sci.* **1994**, *2*, 31.
(14) Morishima, Y. In *Solvents and Self-Organization of Polymers*; Webber, S. E., Tuzar, D., Munk, P., Eds.; Kluwer Academic Publishers: Dordrecht, The Netherlands, 1996; p 331.
(15) Yusa, S.; Kamachi, M.; Morishima, Y. *Langmuir* **1998**, *14*, 6059.
(16) Noda, T.; Morishima, Y. *Macromolecules* **1999**, *32*, 4631.
(17) Morishima, Y.; Nomura, S.; Ikeda, T.; Seki, M.; Kamachi, M. *Macromolecules* **1995**, *28*, 2874.
(18) Morishima, Y. *Bio-Industry* **1995**, *12*, 20.
(19) Morishima, Y. In *Multidimensional Spectroscopy of Polymers: Vibrational, NMR, and Fluorescence Techniques*; Urban, M. W., Provder, T., Eds.; ACS Symposium Series 598; American Chemical Society: Washington, DC, 1995; p 490.
(20) Seki, M.; Morishima, Y.; Kamachi, M. *Macromolecules* **1992**, *25*, 6540.
(21) Morishima, Y.; Tsuji, M.; Seki, M.; Kamachi, M. *Macromolecules* **1993**, *26*, 3299.
(22) Yamamoto, H.; Mizusaki, M.; Yoda, K.; Morishima, Y. *Macromolecules* **1998**, *31*, 3588.
(23) Yamamoto, H.; Morishima, Y. *Macromolecules* **1999**, *32*, 7469.
(24) Yamamoto, H.; Hashidzume, A.; Morishima. Y. *Polym. J.*, in press.
(25) Hashidzume, A.; Yamamoto, H.; Mizusaki, M.; Morishima, Y. *Polym. J.* **1999**, *31*, 1009.
(26) Morishima, Y.; Kobayashi, T.; Nozakura, S. *Polym. J.* **1989**, *21*, 267.
(27) Morishima, Y.; Tominaga, Y.; Nomura, S.; Kamachi, M. *Macromolecules* **1992**, *25*, 861.
(28) Perrin, F. *J. Phys. Radium* **1926**, *7*, 39.
(29) Erdmann, K.; Gutsze, A. *Colloid Polym. Sci.* **1987**, *256*, 667.
(30) Rady, P.; Budd, P. M.; Heatiey, F.; Price, C. *J. Polym. Sci., Polym. Phys. Ed.* **1991**, *29*, 451.
(31) Brereton, M. G.; Ward, I. M.; Boden, N.; Wright, P. *Macromolecules* **1991**, *24*, 2068.
(32) Meiboom, S.; Gill, D. *Rev. Sci. Instrum.* **1958**, *29*, 688.
(33) Jakes, J. *Czech. J. Phys.* **1988**, *B38*, 1305.
(34) Phillies, G. D. J. *Anal. Chem.* **1990**, *62*, 1049A.
(35) Phillies, G. D. J. *J. Chem. Phys.* **1988**, *89*, 91.
(36) Morishima, Y.; Tominaga, Y.; Kamachi, M.; Okada, T.; Hirata, Y.; Mataga, N. *J. Phys. Chem.* **1991**, *95*, 6027.
(37) Kalyanasundaram, K.; Thomas, J. K. *J. Am. Chem. Soc.* **1977**, *99*, 2039.
(38) Kiserow, D.; Chan, J.; Ramireddy, C.; Munk, P.; Webber, S. E. *Macromolecules* **1992**, *25*, 5338.
(39) Chan, J.; Fox, S.; Kiserow, D.; Ramireddy, C.; Munk, P.; Webber, S. E. *Macromolecules* **1993**, *26*, 7016.
(40) Pake, G. E. In *Solid State Physics*; Seitz, F., Turnbull, D., Eds.; Academic Press: New York, 1965; Vol. 2, p 1.

MA9920487